Available online at www.sciencedirect.com
ScienceDirect
Trans. Nonferrous Met. Soc. China 21(2011) 1335−1339
Transactions of Nonferrous Metals Society of China
www.tnmsc.cn

Effects of alkali and heat treatment on strength of porous Ti35Nb

WAN Xiao-jun

Department of Physics and Telecommunication Engineering, Hunan City University, Yiyang 413000, China

Received 13 December 2010; accepted 26 April 2011

Abstract: Porous Ti35Nb alloy with a porosity of 66% was made by a powder metallurgical method, and then it was treated by a standard treatment for activating the surface of Ti implant materials involving alkali and heat treatment. The alkali and heat treatment causes damages of the struts of the porous Ti35Nb in the form of reaction products layer, grain-pullout and cracks. Consequently, it leads to a significant degradation of the strength of the porous alloy. The effect of the alkali and heat treatment on the strength of the porous alloy was discussed.

Key words: porous Ti-Nb alloy; mechanical property; alkali treatment

1 Introduction

The Ti-35%Nb (Ti35Nb) alloy shows a good shape memory effect because of the presence of α'' phase. If we can make the alloys into the porous materials, they will show a good prospect for orthopedic applications due to their biological and mechanical compatibilities with implant materials [1−6]. However, they do not form a direct chemical bonding to host bone tissues in the living body due to the formation of fibrous capsules at the interface, which isolates the implant materials from the surrounding bones and causes desperate failures of implants. The problem can be solved by coating a biologically active bonelike apatite layer on the surfaces of titanium alloys. Therefore, many coating techniques have been developed for the formation of the apatite layer on titanium alloys [7−9]. Of these techniques, biomimetic techniques to deposit bioactive apatite coating on metal substrates have attracted much attention in the last two decades due to their low operation temperature, relatively good bonding strength and the formation of bone-like apatite [10−13]. In these methods, the alkali and heat treatment plays a key role in the formation of apatite layer, because the structural changes of titanium surfaces during the treatment lead to the formation of a bioactive titanate layer containing alkali ions. This layer can accelerate the spontaneous nucleation of a bonelike apatite layer on titanium surface in simulated body fluid (SBF) [14]. However, the studies have mainly concentrated on the formation and the characteristics of apatite coatings on the alkali-treated surfaces of titanium alloys in SBF. To date, there are no systematic studies on the mechanical behaviour changes of the porous material of titanium alloys after the alkali and heat treatment, in spite of the fact that this has an important effect on the bioactivity of the alloy and the bond characteristics of apatite layers deposited subsequently in SBF with titanium substrates. In light of this, porous Ti35Nb (mole fraction) alloy was made by a powder metallurgical method in the present work, and the degradation of the strength of the porous Ti35Nb after alkali treatment in NaOH solutions with different concentrations was evaluated.

2 Experimental

The porous Ti35Nb samples were made by a powder metallurgical method, which was described in details in Refs. [5−6]. The starting materials were commercially available titanium (purity ≥ 99.9%, and powder size ≤45 μm) and niobium (purity ≥ 99.9%, and powder size ≤45 μm) powders. Elemental metal powders of Ti and Nb were mixed together according to the desired composition of Ti-35Nb, and then put in a steel container. The mechanically alloying process was

Foundation item: Project (2010FJ3132) supported by the Scientific and Technological Project of Hunan Science and Technology Commission, China; Project (09A089) supported by the Scientific Research Fund of Hunan Provincial Education Department, China
Corresponding author: WAN Xiao-jun; Tel: +86-15207371668; E-mail: yhqwxj@163.com
DOI: 10.1016/S1003-6326(11)60862-5

conducted in a planetary ball mill (Retsch, PM400) at room temperature. The mass ratio of ball to powder was 20:1. The mixed powders were ball milled at a speed of 200 r/min for 2 h. For fabrication of the porous Ti-35Nb alloy, the ball-milled powders were thoroughly mixed with 40% (mass fraction) ammonium hydrogen carbonate, NH_4HCO_3, as a space-holding material with a particle size of 300−500 μm. The powders were subsequently compacted on a uniaxial cold press machine under the pressure of 500 MPa into green compact bars with dimensions of *d* 10 mm × 13 mm. The green compacts were heated to 175 °C to burn out the spacers in air, and then put into vacuum furnace to sinter at 1 200 °C for 2 h. The sintered samples were washed with ethanol in ultrasonic cleaner, and then dried in an oven at 150 °C. The pore structure was characterized by scanning electron microscopy (SEM). The porosity was measured by the Archimedes method in water based on the following principles: the mass (m_s) of a dried porous bar and the mass (m_x) of the porous bar filled with wax with a density of ρ_x were weighed in air. Then, the open porosity (θ_p) can be calculated by the expression of $\theta_p=(m_x-m_s)/(V_x\rho_x)$. And the overall porosity (θ_v) can be calculated by the expression of $\theta_v=1-m_x/(V_x\rho_t)$, ($\rho_t$=5.32 g/cm^3 [15], which is the theoretical density of the Ti35Nb alloy). The porosity of the as-sintered porous samples was measured to be about 66%.

The sintered samples were immersed in 1, 2 and 5 mol/L NaOH solution at 60 °C for 24 h, and then washed with distilled water in an ultrasonic washer and dried in air. After that, the alkali treated samples were heat treated at 600 °C for 1 h in a vacuum furnace.

The sintered samples were characterized by X-ray diffraction (XRD) on a Rigaku D/Max-rA to identify the phases in the porous Ti35Nb alloy. The compression tests on the as-sintered and the alkali and heat treated samples were conducted on a materials test system (MTS) machine. The dimension of the compression samples were 10 mm in diameter and 12 mm in length, and the initial strain rate was about 10^{-4} s^{-1}.

3 Results and discussion

Figure 1 shows the XRD pattern of the as-sintered sample. The diffraction peaks mainly come from *β*-Ti phase, which implies that the complete alloying is achieved in the porous Ti35Nb alloy after ball milling for 2 h and sintering at 1 200 °C for 2 h. The microstructure of the sintered alloy consists of *β*-Ti, which is similar to the alloy with the same composition made by ingot method [16].

Figures 2(a) and (b) show the optical micrographs of the porous Ti35Nb sample (porosity of about 66%) in transversal and longitudinal sections, respectively. The quantitative image analysis results indicated that the porous sample contains 56.5% open pores and 4.5% closed pores. The result is slightly smaller than that measured by Archimedes method, which may be caused by the fact that there are some micro-pores on the struts. The average pore size in the transversal section is 194 μm with a standard deviation of 110.4 μm. The porous structure in the longitudinal section exhibits subtle differences compared to that in the transversal section, and the average pore size is about 166 μm with a standard deviation of 84.6 μm, reflecting some level of anisotropy of the porosity in the Ti35Nb porous sample.

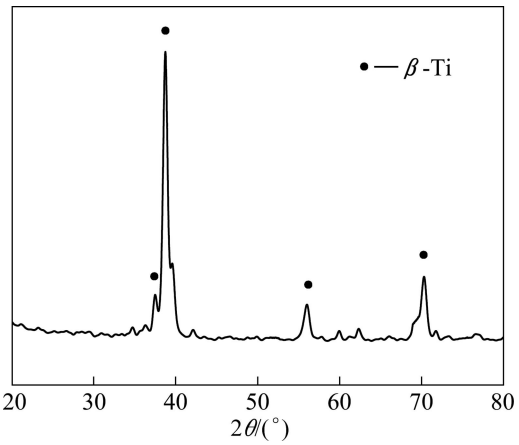

Fig. 1 XRD pattern of porous sample sintered at 1 200 °C for 2 h

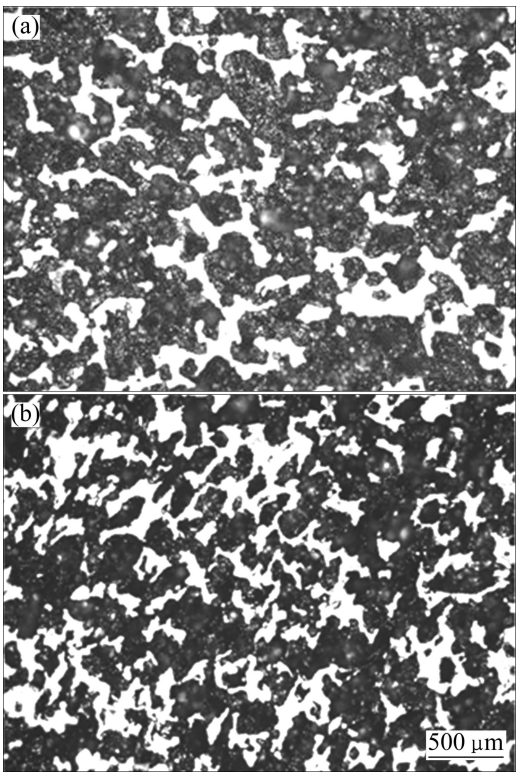

Fig. 2 Optical microstructures of as-sintered porous Ti35Nb alloy: (a) Transversal section; (b) Longitudinal section

Figure 3 shows the SEM images of porous Ti35Nb samples in as-sintered state and after alkali and heat treatment in 1 and 5 mol/L NaOH solutions, respectively. As reported in the previous work [6], the porous Ti35Nb sample contains two types of pores, i.e. small isolated micropores distributed in the wall of the open interconnected macropores induced by the volume shrinkages during the sintering process of the titanium powders, and interconnective macropores created by the space holders, as shown in Fig. 3(a). After the alkali and heat treatment, a layer of corrosion product is visible on the surface of all the samples. By close examination, one can see the evidence of corrosive damage in the form of sharp crack-like pits and grain pullout in several places on the samples (see Fig. 3(d)), and the number and severity of these damaged regions decrease with the decrease of the concentration of alkaline solution (Figs.3(b), (c) and (d)).

The nominal stress—strain curves of the porous samples before and after alkali and heat treatment are shown in Fig. 4. The as-sintered sample exhibits a typical stress—strain curve of porous metals, with an elastic region at the initial stage of deformation, followed by a plateau region where the specimens deform under a constant flow stress (plateau stress). Alkali and heat treatment leads to some changes in the feature of the stress—strain curve of the porous sample. It can be seen that the treated samples exhibit an elastic region, where the stress increases linearly with strain, reaching a peak. After the peak stress, the flow stress decreases slightly followed by the plateau region with a constant flow stress. The plateau stresses (at the strain of 5%) of all the samples were obtained from the graphs, as shown in Fig. 5. It is apparent that the alkali and heat treatment leads to a significant decrease in the plateau stress of the porous Ti35Nb samples irrespective of the concentration of the alkaline solution.

Fundamentally, the mechanical properties of porous metals can be described by the model developed by GIBSON and ASHBY [17]. According to the model, the single most important factor affecting the mechanical properties is the relative density, and the elastic modulus and compressive strength of the porous metals are given by

$$E=C_2E_s(\rho/\rho_s)^2 \quad (1)$$

$$\sigma_{fc}=C_3\sigma_{fs}\ (\rho/\rho_s)^{3/2} \quad (2)$$

where E_s is the elastic modulus of the solid phase; σ_{fs} is the yield strength of the strut material; and C_2 and C_3 are constants. WEN et al applied the model to predict the mechanical properties of the porous titanium with a porosity of 78%, which gave a reasonable agreement to the experimental results [6]. The results in the present work also confirm that the model is valid for the current porous Ti35Nb. It was found that the alkali and heat treatment significantly decreased the strength of the porous material. The reasons lie in the reaction between the alloy substrate and the alkali solution, which may cause the reduction in the relative density of the porous Ti35Nb and the damage of the strut of the pores.

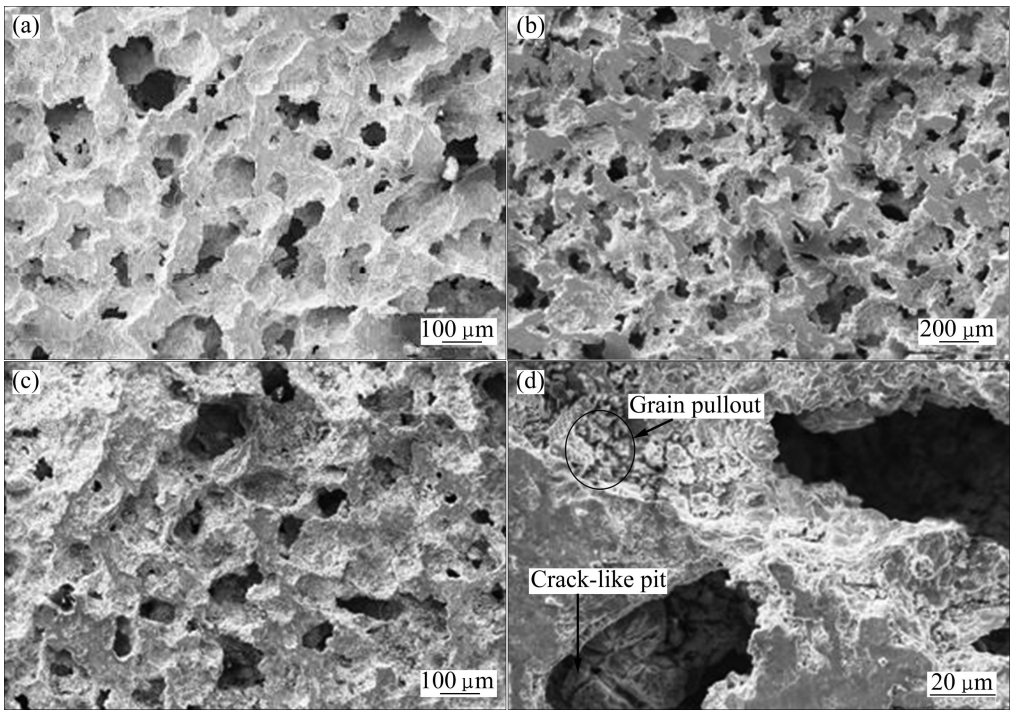

Fig. 3 SEM images of porous Ti35Nb before and after alkali and heat treatment: (a) As-sintered; (b) Alkali treated in 1 mol/L NaOH solution; (c) Alkali treated in 5 mol/L NaOH solution; (d) Enlarged image of (c)

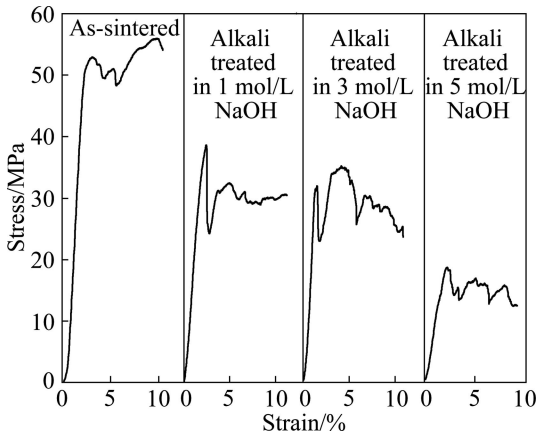

Fig. 4 Nominal stress—strain curves of porous Ti35Nb before and after alkali and heat treatment in different concentrations of NaOH solution

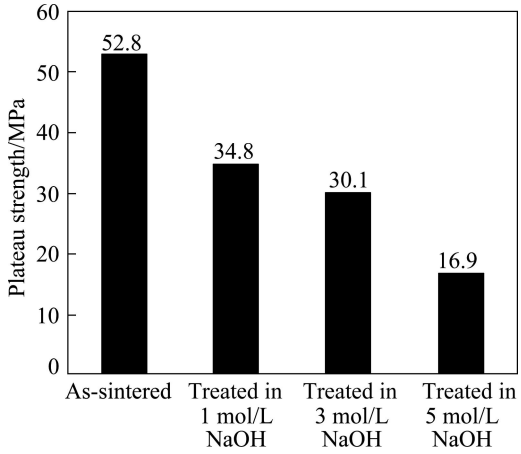

Fig. 5 Plateau stress of porous Ti35Nb before and after alkali and heat treatment

The surface structural changes of titanium during the alkali and heat treatments were reported in previous work [18−22]. During the alkali treatment, the passive TiO_2 layer on the titanium surface partially dissolves into alkaline solution because of the corrosive attack of hydroxyl group [18−19]:

$$TiO_2 + OH^- \rightarrow HTiO_3^- \quad (3)$$

In the mean time, the titanium substrate reacts with the alkaline solution through the following hydration reactions [18, 20−22]:

$$Ti + 3OH^- \rightarrow Ti(OH)_3^+ + 4e^- \quad (4)$$

$$Ti(OH)_3^+ + e^- \rightarrow TiO_2 \cdot H_2O + \frac{1}{2} H_2\uparrow \quad (5)$$

$$Ti(OH)_3^+ + OH^- \rightleftharpoons Ti(OH)_4 \quad (6)$$

A further hydroxyl attack to hydrated TiO_2 will produce negatively charged hydrates on the surfaces of the substrates as follows:

$$TiO_2 \cdot nH_2O + OH^- \rightleftharpoons [HTiO_3]^- \cdot nH_2O \quad (7)$$

These negatively charged species are combined with alkali ions in the aqueous solution, resulting in the formation of an alkali titanate hydrogel layer [23]. During the heat treatment, the hydrogel layer is dehydrated and densified to form a stable amorphous or crystalline alkali titanate layer.

The chemical reactions mentioned above cause the thinning of the struts of porous Ti35Nb, resulting in the decrease of the relative density (ρ/ρ_s) of the treated samples compared to the as-sintered sample. In the present work, the relative density (ρ/ρ_s) of the samples after the alkali and heat treatments was measured by the Archimedes method, and the values are about 68%, 70% and 74% for the samples alkali treated in 1, 3 and 5 mol/L NaOH solutions, respectively. Consequently, based on the model by Gibson and Ashby, it gives rise to a sample with weaker mechanical strength after alkali and heat treatment.

Moreover, although there is little knowledge about the effect of strut surface condition on the properties of porous metals, it is reasonable to assume that the quality of the surfaces in a corroded porous metal will be compromised to affect the overall mechanical properties. This is because, in the porous metals, the dominant deformation mode initiates at strut surfaces where the local strain is the largest during strut bending, and most deformation, at least at low strains, is concentrated on the struts. Therefore, for the struts with a low thickness, the surface effects are crucially important to their mechanical properties. The present results indicate that the corrosive damage due to the aggressive alkali solution attack may extend beyond the surfaces in certain cases, such as grain pullout, severe pitting, or crack. It may make the strut brittle and degrade the strength of the strut, thus deteriorate the overall mechanical properties of the porous Ti35Nb alloy.

4 Conclusions

1) The porous Ti35Nb with a porosity of 66% was successfully made by a powder metallurgical method. The average pore sizes in the transversal section and the longitudinal section are 194 and 166 μm, respectively. The strength of the porous alloy is about 52.8 MPa.

2) The porous alloy was treated by a standard treatment for activating the surface of Ti implant materials involving alkali and heat treatment. The alkali and heat treatment led to damage of the strut of the porous metals in the forms of reaction products layer, grain pullout and cracks.

3) The strengths of the porous Ti35Nb alloys after the alkali treatment in 1, 3 and 5 mol/L NaOH solutions and heat treatment are 34.8, 30.1 and 16.9 MPa, respectively. The degradation of the strength of the

porous Ti35Nb can be attributed to the reactions between the titanium substrate and the alkali solution, which leads to thinning and corrosive damages of the struts of the porous Ti35Nb alloy.

References

[1] DAVIS N G, TEISEN D J, SCHUH C, DUNAND D C. Solid-state foaming of titanium by superplastic expansion of argon-filled pores [J]. Journal of Materials Research, 2001, 16(5): 1508−1519.

[2] WEN C E, YAMADA Y, SHIMOJIMA K, CHINO Y, HOSOKAWA H, MABUCHI M. Novel titanium foam for bone tissue engineering [J]. Journal of Materials Research, 2002, 17(10): 2633−2639.

[3] NAKAJIMA H, IKEDA T, HYUN S K. Fabrication of lotus-type porous metals and their physical properties [J]. Advanced Engineering Materials, 2004, 6(6): 377−384.

[4] DUNCAND D C. Processing of titanium foams [J]. Advanced Engineering Materials, 2004, 6(6): 369−376.

[5] WEN C E, YAMADA Y, SHIMOJIMA K, CHINO Y, ASAHINA T, MABUCHI M. Processing and mechanical properties of autogenous titanium implant materials [J]. Journal of Materials Science: Materials in Medicine, 2002, 13(4): 397−401.

[6] WEN CE, MABUCHI M, YAMADA Y, SHIMOJIMA K, CHINO Y, ASAHINA T. Processing of biocompatible porous Ti and Mg [J]. Scripta Materialia, 2001, 45(10): 1147−1153.

[7] KLEIN C P A T, PATKA P, van der LUBBE H B M, WOLKE J G C, de GROOT K. Plasma-sprayed coatings of tetracalciumphosphate, hydroxyl-apatite, and α-TCP on titanium alloy: An interface study [J]. Journal of Biomedical Materials Research, 1991, 25(1): 53−65.

[8] COTELL C M, CHRISEY D B, GRABOWSKI K S, SPRAGUE J A, GOSSETT C R. Pulsed laser deposition of hydroxylapatite thin films on Ti-6Al-4V [J]. Journal of Applied Biomaterials, 1992, 3(2): 87−93.

[9] LIU D M, YANG Q, TROCZYNSKI T. Sol-gel hydroxyapatite coatings on stainless steel substrates [J]. Biomaterials, 2002, 23(3): 691−698.

[10] KIM H M, MIYAJI F, KOKUBO T, NAKAMURA T. Effect of heat treatment on apatite-forming ability of Ti metal induced by alkali treatment [J]. Journal of Materials Science: Materials in Medicine, 1997, 8(6): 341−347.

[11] OHTSUKI C, IIDA H, HAYAKAWA S, OSAKA A. Bioactivity of titanium treated with hydrogen peroxide solutions containing metal chlorides [J]. Journal of Biomedical Materials Research, 1997, 35(1): 39−47.

[12] LI F, FENG Q L, CUI F Z, LI H D, SCHUBERT H. A simple biomimetic method for calcium phosphate coating [J]. Surface and Coatings Technology, 2002, 154(1): 88−93.

[13] WEN H B, de WIJN J R, CUI F Z, de GROOT K. Preparation of bioactive Ti6Al4V surfaces by a simple method [J]. Biomaterials, 1998, 19(1−3): 215−221.

[14] KIM H M, MIYAJI F, KOKUBO T, NAKAMURA T. Preparation of bioactive Ti and its alloys via simple chemical surface treatment [J]. Journal of Biomedical Materials Research, 1996, 32(3): 409−417.

[15] LIN J G, ZHANG Y F, MA M. Preparation of porous Ti35Nb alloy and its mechanical properties under monotonic and cyclic loading [J]. Transactions of Nonferrous Metals Society of China, 2010, 20(3): 390−394.

[16] ZHANG D C, LIN J G, JIANG W J, MA M, PENG Z G. Shape memory and superelastic behavior of Ti-7.5Nb-4Mo-1Sn alloy [J]. Materials & Design, 2011, 32(8−9): 4614−4617.

[17] GIBSON L J, ASHBY M F. Cellular solids: Structure and properties [M]. Cambridge: Cambridge University Press, 1997: 96−97.

[18] ARSOV L D, KORMANN C, PLIETH W. Electrochemical synthesis and in situ Raman spectroscopy of thin films of titanium dioxide [J]. Journal of Raman Spectroscopy, 1991, 22(10): 573−575.

[19] PRUSI A R, ARSOV L D. The growth kinetics and optical properties of films formed under open circuit conditions on a titanium surface in potassium hydroxide solutions [J]. Corrosion Science, 1992, 33(1): 153−164.

[20] HURLEN T, WILHELMSEN W. Kinetics of the $Fe(CN)_{3-6}$/$Fe(CN)_{4-6}$ couple at passive titanium electrodes [J]. Electrochimica Acta, 1988, 33(12): 1729−1733.

[21] TENGVALL P, LUNDSTROM I. Physico-chemical considerations of titanium as a biomaterial [J]. Clinical Materials, 1992, 9(2): 115−134.

[22] HEALY K E, DUCHEYNE P. Oxidation kinetics of titanium thin films in model physiologic environments [J]. Journal of Colloid and Interface Science, 1992, 150(2): 404−417.

[23] CHEN X B, NOURI A, HODGSON P D, WEN C E. Surface modification of TiZr alloy for biomedical application [J]. Advanced Materials Research, 2006, 15−17: 89−94.

碱处理及热处理对 Ti35Nb 多孔合金强度的影响

万小军

湖南城市学院 物理与电子工程系，益阳 413000

摘 要：采用粉末冶金法制备孔隙率为 66%的 Ti35Nb 多孔合金，并用标准的碱处理和热处理方法对该多孔合金进行表面活性处理，研究表面活性处理对多孔合金孔结构和力学性能的影响。结果表明，碱处理对多孔合金孔壁有很强的腐蚀作用，在孔壁上产生了微裂纹和颗粒脱落等缺陷，这些缺陷导致多孔合金的强度显著下降。

关键词：Ti-Nb 多孔合金；力学性能；碱处理

(Edited by YUAN Sai-qian)